Reward-Sensitive Basal Ganglia Stabilize the Maintenance of Goal-Relevant Neural Patterns in Adolescents

Nicholas A. Hubbard[1,2], **Rachel R. Romeo**[1,3], **Hannah Grotzinger**[1], **Melissa Giebler**[1], **Andrea Imhof**[1,4], **Clemens C. C. Bauer**[1], **John D. E. Gabrieli**[1]

[1]Massachusetts Institute of Technology

[2]University of Nebraska-Lincoln

[3]Harvard Medical School

[4]University of Oregon

Abstract

Maturation of basal ganglia (BG) and frontoparietal circuitry parallels developmental gains in working memory (WM). Neurobiological models posit that adult WM performance is enhanced by communication between reward-sensitive BG and frontoparietal regions, via increased stability in the maintenance of goal-relevant neural patterns. It is not known whether this reward-driven pattern stability mechanism may have a role in WM development. In 34 young adolescents (12.16–14.72 years old) undergoing fMRI, reward-sensitive BG regions were localized using an incentive processing task. WM-sensitive regions were localized using a delayed-response WM task. Functional connectivity analyses were used to examine the stability of goal-relevant functional connectivity patterns during WM delay periods between and within reward-sensitive BG and WM-sensitive frontoparietal regions. Analyses revealed that more stable goal-relevant connectivity patterns between reward-sensitive BG and WM-sensitive frontoparietal regions were associated with both greater adolescent age and WM ability. Computational lesion models also revealed that functional connections to WM-sensitive frontoparietal regions from reward-sensitive BG uniquely increased the stability of goal-relevant functional connectivity patterns within frontoparietal regions. Findings suggested (1) the extent to which goal-relevant communication patterns within reward-frontoparietal circuitry are maintained increases with adolescent development and WM ability and (2) communication from reward-sensitive BG to frontoparietal regions enhances the maintenance of goal-relevant neural patterns in adolescents' WM. The maturation of reward-driven stability of goal-relevant neural patterns may provide a putative mechanism for understanding the developmental enhancement of WM.

INTRODUCTION

Structural and functional connections within cortico-basal ganglia (BG) circuitry are still developing during adolescence (Insel, Kastman, Glenn, & Somerville, 2017; Heller, Cohen, Dreyfuss, & Casey, 2016; Simmonds, Hallquist, Asato, & Luna, 2014; Lebel &

Beaulieu, 2011). Greater volume and strength of anatomical connections between BG and frontoparietal regions are predictive of age-related increases in working memory (WM) performance across youth and young adults (Darki & Klingberg, 2015). These regions also demonstrate age-related, performance-related, and longitudinal changes to functional responses during WM in developmental imaging studies (Simmonds, Hallquist, & Luna, 2017; Ullman, Almeida, & Klingberg, 2014; Satterthwaite et al., 2012). However, the precise role of cortico-BG circuitry in WM development is not known. We hypothesized that communication between reward-sensitive BG and WM-sensitive frontoparietal regions is fundamental for enhancing the maintenance of goal-relevant representations during adolescent development. To investigate this hypothesis, fMRI was used in a group of young adolescents. The stability of goal-relevant functional connectivity patterns was assessed during WM delay periods between and within reward-sensitive BG and WM-sensitive frontoparietal regions.

WM ability improves from childhood to young adulthood (Nemmi et al., 2018; Simmonds et al., 2017; Ullman et al., 2014; Brockmole & Logie, 2013; Satterthwaite et al., 2012, 2013; Crone, Wendelken, Donohue, Van Leijenhorst, & Bunge, 2006; Cowan et al., 2005; Gathercole, Pickering, Ambridge, & Wearing, 2004; Barrouillet & Camos, 2001; Towse, Hitch, & Hutton, 1998). The exact neural mechanisms contributing to age-related improvements in WM are not known. However, neural correlates exist between functions and structures of the developing brain and WM (Davidow, Insel, & Somerville, 2018; Crone & Steinbeis, 2017; Luna, Marek, Larsen, Tervo-Clemmens, & Chahal, 2015). In developmental studies, functional imaging has revealed age-related, performance-related, and longitudinal changes in BG and frontoparietal responses during WM performance. For example, across a sample of 8- to 22-year-olds performing an *n*-back task, ventral BG BOLD activations were shown to peak in adolescent participants (around ages 14–15 years; Satterthwaite et al., 2012). In a sample spanning 6- to 20-year-olds, positive associations were observed between WM capacity and frontoparietal BOLD activations during a visuospatial WM task (Ullman et al., 2014). In this same study, increased BOLD activations in BG and thalamus were also predictive of developmental enhancement of WM performance 2 years later. Furthermore, one study examined BOLD activations across development using a delayed-response task designed to isolate during different WM phases (i.e., encoding, delay, retrieval [Rypma & D'Esposito, 1999]; Simmonds et al., 2017). Here, WM delay-period activations in BG and certain frontoparietal regions both showed significant changes in activation as youth aged from early to mid-adolescence (Simmonds et al., 2017).

Models of the adult brain may offer one possible explanation for the combined significance of BG and frontoparietal regions in adolescent WM development. Neurobiological models of adult WM postulate that communication between reward-sensitive BG (e.g., ventral BG) and frontoparietal regions enhances the maintenance of goal-relevant representations in WM (Frank & Badre, 2011; O'Reilly, Herd, & Pauli, 2010; Reynolds & O'Reilly, 2009; Gruber, Dayan, Gutkin, & Solla, 2006; O'Reilly & Frank, 2006; see also O'Doherty et al., 2014; Atallah, Lopez-Paniagua, Rudy, & O'Reilly, 2007). Specifically, communication from reward-sensitive BG to prefrontal and posterior (e.g., parietal) regions enhances the "stability," or consistency, of encoded goal-relevant neural patterns during WM-delay

periods (Frank & Badre, 2011; Gruber et al., 2006; O'Reilly & Frank, 2006; cf. Li, Lindenderber, & Bäckmann, 2010; Li, Lindenberger, & Sikström, 2001; Durstewitz, Seamans, & Sejnowski, 2000). In turn, greater stability of goal-relevant neural patterns during WM-delay periods enhances performance by making goal-relevant circuits more easily activated during retrieval cueing (Murray et al., 2017; Stokes, 2016; Lansink et al., 2008; Mongillo, Barak, & Tsodyks, 2008; Durstewitz et al., 2000; cf. Ezzyat & Davachi, 2014; Tambini & Davachi, 2013; Hasselmo & Giocomo, 2006). Because cortico-BG activations and communication pathways are still maturing during adolescence (Insel et al., 2017; Heller et al., 2016; Simmonds et al., 2014; Lebel & Beaulieu, 2011), age-related or individual variation in brain development may influence the ability for reward-sensitive BG to stabilize goal-relevant neural patterns (cf. Zhou, Salinas, Stanford, & Constantinidis, 2016; Zhou et al., 2016).

Although broader BG and frontoparietal responses during WM change with age and are related to WM performance in developmental samples (Simmonds et al., 2017; Ullman et al., 2014; Satterthwaite et al., 2012), evidence for a mechanism explaining the combined significance of these regions in WM development has not yet been demonstrated. Moreover, reward-sensitive BG demonstrate functional and anatomical differences in adolescents compared to children and adults, and these regions undergo significant developmental changes in function and structure at least until young adulthood (Davidow et al., 2019; Schrueuders et al., 2018; Wierenga et al., 2018; Satterthwaite et al., 2012, 2013; Somerville, Hare, & Casey, 2011; see also Casey et al., 2018; Davidow et al., 2018; Larsen & Luna, 2018; Luna et al., 2015). To examine reward-driven pattern stability as one possible explanation for BG and frontoparietal regions' apparent combined role in adolescent WM, this study used fMRI in 34 young adolescents to examine functional connections between reward-sensitive BG and WM-sensitive frontoparietal regions, during a WM task. Combining functional activations from an incentive processing and delayed-response task allowed us to independently localize reward-sensitive BG regions that were active during WM performance. The event-related, delayed-response task also allowed us to isolate putative changes in functional connectivity during WM encoding and delay periods (Rissman, Gazzaley, & D'Esposito, 2004).

We tested whether the stability of goal-relevant functional connectivity patterns between reward-sensitive BG and WM-sensitive frontoparietal regions was related to adolescent WM development by assessing its correlations with age and WM ability, as measured by a latent variable of WM performance. Computational lesion modeling was also used to examine one mechanism by which reward-sensitive BG are hypothesized to enhance adult WM. Specifically, lesion modeling tested whether adolescents' communication signals from reward-sensitive BG increased the stability of goal-relevant neural patterns maintained within WM-sensitive frontoparietal regions (Frank & Badre, 2011; O'Reilly et al., 2010; Reynolds & O'Reilly, 2009; Gruber et al., 2006; O'Reilly & Frank, 2006).

METHODS

Participants and Procedure

Thirty-six young adolescents were recruited through social media, fliers, and local schools to participate in this study. Two adolescents failed to meet a priori defined criteria on the prescan delayed-response WM task (WM capacity score of at least 3 [see below]); thus, relevant brain imaging data were not collected from these individuals. Thirty-four participants received the entire study protocol and were used in analyses detailed here ($n = 34$, $M_{age} = 13.72$ [$SEM = 0.102$, range = 12.16–14.72], 58.82% female). Three parents reported their adolescent's use of psychostimulant medication for attention-deficit hyperactivity disorder (ADHD) (8.8%), which may affect reward-sensitive BG responses or functional connections (Dukart et al., 2018). Written consent was obtained from an accompanying parent, and assent was obtained from the adolescent. Sample size and age groups were determined based on similar, adolescent WM imaging studies performed in our laboratory (Finn et al., 2016; Leonard, Mackey, Finn, & Gabrieli, 2015). Primary inclusion criteria included seventh or eighth grade student at a public school, English proficiency, and accompanying parent English and/or Spanish proficiency. Primary exclusion criteria included MR contraindications, history of autism spectrum disorder or neurological disability, or premature birth (< 34 weeks). Procedures were approved by the Massachusetts Institute of Technology Committee on the Use of Human Subjects. Parents and adolescents were compensated for their time.

This study was part of a larger project investigating factors influencing middle-school brain development and achievement. For brevity, only study-specific procedures are detailed here. Adolescents completed four WM tasks ([1] prescan and [2] in-scanner delay-response tasks, [3] count span, and [4] *n*-back) and an incentive processing task (IPT). Tasks were presented using PsychoPy2 software (Pierce, 2007). Participants were trained on how to complete tasks before executing the actual tasks. For tasks presented within the MR environment, participants were given additional opportunities for explanation on task instructions before commencing scanning.

Prescan and In-scanner Delayed-Response WM Tasks

We employed two Sternberg-type, delayed-response WM tasks (Sternberg, 1966), which were consistent with similar paradigms used across the lifespan (Simmonds et al., 2017; Hubbard et al., 2014; Rissman et al., 2004; Rypma & D'Esposito, 1999, 2000; Rypma, Prabhakaran, Desmond, Glover, & Gabrieli, 1999; see Daniel, Katz, & Robinson, 2016). The first WM task was given to adolescents before scanning. This prescan delayed-response WM task estimated adolescents' WM capacities. Estimated WM capacities were then used to calibrate the second, in-scanner delayed-response WM task (Shah et al., 2019). By individually calibrating demand for the in-scanner delayed-response WM task, we attempted to ensure that adolescents' WM abilities were sufficiently challenged and that individual differences in performance and activations were not inflated by the demands of this task (Davidow et al., 2018). For instance, reward-sensitive BG activations in developmental samples are increased on accurate relative to inaccurate WM trials (Satterthwaite et al., 2012). Using a WM task with standard demand conditions could bias lower-ability

adolescents to have fewer accurate responses relative to high-ability adolescents, unduly affecting activation in reward-sensitive BG. Conversely, reward-sensitive BG activation to accurate responses increases with more challenging demand conditions, demonstrating that accurate responses to more challenging conditions result in greater activations in reward-sensitive BG (Satterthwaite et al., 2012).

Prescan Delayed-Response WM Task—The prescan WM task presented participants with lists of three to seven letters (i.e., goal-relevant stimuli), which participants needed to remember over an 8-sec delay period. Participants were then asked to register a binary response to a retrieval cue (Figure 1A). Each list size of goal-relevant information was presented seven times for 35 trials. Participants were instructed to emphasize speed and accuracy in their responding to the retrieval cue. The prescan WM task approximated WM capacity by adapting a standard formula (McNab & Klingberg, 2008; Cowan, 2001). Here, $K = S(H - FA)$, where S was the largest list size that the participant could achieve with > 50% recognition accuracy, H reflected correct detections (i.e., hits), and FA reflected false detections (i.e., false alarms; Shah et al., 2019). WM capacity estimates from this task indicated a mean of 5.32 goal-relevant stimuli (see Table 1) could be reliably remembered over the delay period. This estimate is consistent with other reports of youth and young adolescents' WM capacities (Barrouillet & Camos, 2001; Towse et al., 1998).

In-scanner Delayed-Response WM Task—WM capacity estimates were used to calibrate the in-scanner WM task, which was identical to the prescan WM task, except (1) intertrial intervals were jittered at 9, 10, or 11 sec to accommodate hemodynamic responses; (2) to-be-remembered list sizes were calibrated based on each participant's WM capacity estimate (three demand conditions: two letters, K letters, and $K + 1$ letters); (3) 10 trials were added to this task to enhance the reliability of the fMRI signal; and (4) the task was broken into four runs to allow for numerous opportunities for short rests and communication between the MR operator and the adolescent. Participants completed 45 trials of this paradigm, which were equally distributed across demand conditions. Time to complete four runs of this task took approximately 20 min. Average percentage of accurate responses and average RTs from this task were used in subsequent analyses.

Additional WM Tasks and Latent Variable Construction

Count Span—This task required participants to remember the number of target shapes in an array while ignoring irrelevant shapes (Cowan et al., 2005). After n arrays ($n = 1$–6), participants were instructed to recall the number of targets, per array, in the order that these arrays were presented. There were 18 trials (three per array size). Percentage of accurate trials was used as our primary variable of interest from the count-span task.

n-Back—This task presented a single white letter on a black screen, back-projected within the scanner. Participants were trained to press a button every time the letter on the current screen matched one presented one or two letters preceding the current letter (1-back, 2-back). For the 0-back condition, participants were instructed to respond every time the letter "W" was presented on the screen (Finn et al., 2016). Percentage of accurate trials and RTs were used as the primary variables of interest from the *n*-back task.

Latent WM Variable—The objective of the latent variable was to quantify common variance between the measures of WM performance to create a single component that was more representative than any individual measure of our participants' general WM ability (see Cowan et al., 2005). A latent variable was created from six outputs of all four WM tasks using principal component analysis (PCA). The outputs chosen are in Tables 1 and 2. RT for count span was not used in these analyses because trial-level variation in RT was high (range = 0.48–25 sec), and thus, we assumed that variance accounted for by individual differences in WM ability in this measure was obfuscated by other factors (e.g., individual differences in one's typing proficiency). Neither RT nor percent accuracy from the prescan WM task was included in latent variable analyses. The prescan WM task was designed to challenge most participants with list sizes well beyond their capabilities; thus, an aggregate measure of accuracy or RT might not yield an accurate assessment of WM ability (Baddeley, Logie, Bressi, Della Salla, & Spinnler, 1986).

Mahalanobis distance was used to test for potential multivariate outliers across the six selected WM performance measures. One participant (Mahalanobis distance = 3.64 *SD*s) fell beyond the 95% upper confidence limit of the multivariate distribution (3.36). This multivariate outlier was excluded from the PCA and subsequent WM performance analyses. One participant was also excluded from these analyses because they had no evidence of a registered response for the entirety of the *n*-back task.

IPT

The IPT was adapted from the Human Connectome Project (Barch et al., 2013). Reward conditions in IPTs reliably activate youth and adult ventral BG (Speer, Bhanji, & Delgado, 2014; Forbes et al., 2009; May et al., 2004; Tricomi, Delgado, & Fiez, 2004; Delgado, Nystrom, Fissell, Noll, & Fiez, 2000; Figure 1B). This IPT has also been shown to activate adolescent ventral BG (Hubbard et al., 2020). Before the task began, participants were informed that their responses would result in winning or losing actual money. During scanning, participants guessed via button presses whether a to-be-revealed number (between 1 and 9) was greater than or less than 5. Participants then received an image of the actual number and visual feedback regarding whether they had guessed correctly. During reward conditions, participants were informed they guessed correctly and were shown that they would have $1 added to their task winnings. During loss conditions, participants were informed they guessed incorrectly and that they would have $0.50 deducted from their task winnings. Loss trials were half of the magnitude of reward trials to account for greater sensitivity of participants to loss compared to reward (e.g., Tversky & Kahneman, 1991). If the participant failed to respond in the time allotted by the trial, the participant was shown that he or she did not win or lose money for that trial. The number of reward and loss trials was experimentally controlled so that each 28-sec block featured primarily reward or primarily loss trials; thus, all participants received the same number of reward and loss blocks and the same task compensation. There were eight trials per block. There were two types of experimental blocks (28 sec/block) and a brief fixation period in between blocks (3 sec). Block conditions were balanced and pseudorandomized across two runs. Each block type (reward, loss) was presented four times (two times/run). Time to complete two runs of this task was approximately 4 min.

Image Acquisition and Processing

Images were collected using a Siemens Prisma 3-T scanner with a 64-channel head coil. Human Connectome Project acquisition sequences were used (Van Essen et al., 2012; cmrr.umn.edu/multiband). Head cushions were used to limit participant head movement. Participants were trained during a mock scanning session to hold still during MRI acquisition and repeatedly reminded not to move during scanning. Participants were given a finger pad, placed in their dominant hand, to register responses to fMRI tasks.

One high-resolution, multiecho, magnetization-prepared rapid gradient echo T1w image was acquired along with an additional vNav setter for prospective motion correction. The vNav-enabled scan estimated motion throughout the T1w scan and reacquired/replaced *k*-space data unduly affected by motion (Tisdall et al., 2012). T1w scans featured a 0.8-mm isotropic voxel size with 320 slices, acquired in the sagittal orientation, repetition time (TR)/echo time = 4000/1.06 msec. Task fMRI images were acquired using 2-D, multiband, gradient-recalled EPI. Sequences offered a 2.0-mm isotropic voxel size with whole-brain coverage from 72 oblique, axial slices, with TR/echo time = 800/37 msec and flip angle = 52°. Tasks acquired an even number of runs, with two different phase encoding directions (i.e., anterior–posterior [AP], posterior–anterior [PA]). AP–PA spin echo field maps were also acquired for additional distortion correction.

Anatomical and functional images were preprocessed using *fmriprep* (v.1.1.4), including T1 bias-field correction, brain extraction, normalization to the ICBM 152 nonlinear template, tissue segmentation, and motion correction procedures (Esteban et al., 2019). Normalized and extracted functional images were then spatially smoothed using a 6-mm FWHM Gaussian kernel. Functional frames were censored via AFNI's *1d_tool.py* (Cox, 1996) Euclidean-norm approach with a head-displacement threshold comparable to that previously shown appropriate for youth fMRI studies (0.7 mm; Church, Bunge, Petersen, & Schlaggar, 2017; Siegel et al., 2014). Participant runs with fewer than 80% of volumes retained after censoring (Simmonds et al., 2017) were dropped for that participant (three runs at the participant level were dropped in total for the WM task; 0 runs were dropped from the IPT). General linear models (GLMs) were used to estimate task activation and connectivity. All GLMs employed controlled for 6-degrees-of-freedom motion estimates, frame-wise displacement, and censored frames (volume > 0.7-mm head displacement). GLMs also employed AFNI's automatic (high-pass) temporal filtering, to limit temporal tends, including those that may induce autocorrelations, via polynomial detrending with the exponent determined by the integer value of 1 + (Number of TRs/150). Four variables quantifying individual differences in head motion were also used as covariates in target analyses, which also help to control for individual factors influencing autocorrelation; these included average frame-wise displacement across runs (e.g., Satterthwaite et al., 2012), maximum frame-wise displacement across runs, average number of censored frames per run, and maximum number of censored frames per run.

Task Activations and Functional ROIs

To obtain reward- and WM-sensitive functional ROIs, voxel time-series data were convolved with a boxcar impulse response function using the GLMs described above. For the IPT,

reward and loss 28-sec blocks were modeled as separate regressors. For the delayed-response WM task, a task-versus-rest 18-sec boxcar regressor was used in WM activation analyses to derive ROIs active during the WM task. WM functional ROIs were derived using activations from this single task-versus-rest model to avoid biasing our target WM-phase-specific connectivity analyses.

Reward-Sensitive BG ROIs—A reward node was created that was significantly responsive to both reward and WM stimuli. This reward node was determined based on contiguous IPT and WM task activations. For the IPT, we assessed which regions were significantly ($p < .0025$; k 100; FWE rate [FWER]-corrected $ps < .05$) more active during reward blocks relative to loss blocks (Barch et al., 2013; Delgado et al., 2000). For the WM task, we assessed which regions were significantly ($p < .001$; k 70; FWER-corrected $ps < .05$) more active during WM blocks relative to rest periods. A slightly less stringent p value was used for the IPT to account for the lower signal assumed by using the task-versus-task contrast (i.e., reward > loss) and larger extent of activation criterion (i.e., k 100), relative to the task-versus-rest contrast of the WM task (i.e., task > baseline; k 70). The reward node was delineated from clusters with 100 significantly active voxels overlapping from both tasks (Figure 3).

WM-Sensitive Frontoparietal ROIs—We selected clusters of significantly active voxels during the delayed-response WM task, with centers of mass located within lateral prefrontal and posterior parietal regions (z 5, k 25; Figures 2 and 3A). Note that a higher threshold was used here (see also below) compared to the reward-sensitive BG regions to ensure spatial independence between functional ROIs.

Other WM-Sensitive ROIs—WM is a distributed process in the brain (Christophel, Klink, Spitzer, Roelfsema, & Haynes, 2017). Moreover, adolescent development is related to broad-spread changes in brain function during WM and a general tendency for brain activations to become more stable with increasing age (Montez, Calabro, & Luna, 2017; Simmonds et al., 2017). To test alternative hypotheses, we also examined other WM-sensitive brain regions active during the WM task. This circuit included all other, non-frontoparietal, WM-sensitive regions (z 5, k 25; Figures 2 and 3B). These nodes comprised what we termed an "additional WM circuit." This term was not meant to minimize the importance of these regions in WM (e.g., Christophel et al., 2017); rather, it is used to signify that these regions are supplementary to our primary hypotheses.

There was no voxel or anatomical contiguity between ROIs (Figure 3). For instance, one cluster of voxels ($x = -32$, $y = 4$, $z = 0$; 25 voxels; left claustrum/insula/dorsomedial putamen) was not included in these analyses because it was anatomically contiguous with both voxels from the IPT reward contrast and the WM task but did not qualify for the reward node because of its small size. Thus, this cluster was not included in subsequent analyses.

Functional Connectivity Between Functional ROIs

To estimate WM-phase-specific functional connectivity, trial-by-trial activations during encoding, delay, and retrieval periods were modeled as separate regressors by convolution

with canonical, double-gamma impulse response functions. To minimize co-linearity between conditions in the design of our WM task, condition onsets were spaced 4–8 sec apart such that the encoding phase began at the beginning of the trial, the delay phase began 4 sec after the onset of the encoding phase, and the retrieval phase began 8 sec after the onset of the delay phase (see Figure 1). This spacing followed guidelines (4–6 sec when using canonical impulse response functions) from extant event-related research using GLM-based models to recover distinct activations or functional connectivity patterns during different WM conditions (e.g., Rissman et al., 2004; Zarahn, Aguirre, & D'Espositio, 1997). These GLMs used the same nuisance regressors as the GLMs described above. Although retrieval period regressors were not used in subsequent analyses, these periods were modeled to limit "active" hemodynamic contamination of the modeled baseline period. To increase power, target analyses collapsed across WM-demand conditions. WM-phase-specific functional connectivity was estimated using the beta-series method, which has been shown to produce phase-specific connectivity changes during this task (Rissman et al., 2004). This trial-by-trial deconvolution approach has also been successfully applied to assess posten-coding, neural pattern stability in adult episodic memory (Ezzyat & Davachi, 2014; Tambini & Davachi, 2013), and this approach is recommended for fMRI pattern analyses (Mumford, Turner, Ashby, & Poldrack, 2012). Average estimates of WM-phase-specific functional connectivity were obtained using Pearson correlations of beta series (Rissman et al., 2004) between functional ROIs (detailed above). Correlations between these regions were used in functional connectivity pattern stability analyses (detailed below).

Functional Connectivity Pattern Stability

The stability (i.e., less change = greater stability) of goal-relevant functional connectivity patterns between functional ROIs was examined from when goal-relevant patterns were encoded and during the WM-delay period. To quantify functional connectivity pattern stability in a given circuit, the average change (Euclidean distance) of beta-series correlation coefficients was assessed between encoding (e) and delay (d) WM phases. This analytic approach is similar to representational dissimilarity pattern analyses (Connolly et al., 2012; Kriegeskorte, Mur, & Bandettini, 2008). However, instead of trying to identify unique patterns in space, the present approach identified individual differences in neural patterns in time (across memory phases; e.g., Tambini & Davachi, 2013). Pattern stability estimates were Fisher ($atan^{-1}$) transformed to retain a normal distribution across participants (Ezzyat & Davachi, 2014; Tambini & Davachi, 2013). Functional connectivity pattern stability for a given region i, in a circuit of n regions, is formalized as

$$PS = atan^{-1}\left(1 - \left(\frac{\sqrt{(e_{i,1} - d_{i,1})^2 + \ldots (e_{i,n} - d_{i,n})^2}}{n - 1}\right)\right) \quad (1)$$

Higher *PS* indicated that the average pattern of functional connections for a given region, within a given circuit, changed less from when goal-relevant information was encoded to when this information needed to be maintained (see Figure 4 for circuits).

Computational Lesion Approach

The computational lesion approach was adapted from previous research in complex systems science (De Asis-Cruz, Bouyssi-Kobar, Evangelou, Vezina, & Limperopoulos, 2015; Achard, Salvador, Witcher, Suckling, & Bullmore, 2006; Albert, Jeong, & Barabási, 2000). Computational lesion modeling allowed us to ask: What happens to pattern stability in a target circuit if we remove the functional connectivity (i.e., lesion) between each node in this target circuit and an external, target (i.e., lesioned) node? Specifically, this modeling was used to test whether adolescents' communication signals (operationalized by the strength of their functional connectivity) from reward-sensitive BG influenced the stability of goal-relevant neural patterns within WM-sensitive frontoparietal regions (cf. Frank & Badre, 2011; O'Reilly et al., 2010; Reynolds & O'Reilly, 2009; Gruber et al., 2006; O'Reilly & Frank, 2006). Similar to other investigations in the adult and developing brain, computational lesions were applied to our actual data (De Asis-Cruz et al., 2015; Achard et al., 2006). Computational lesioning adapted Equation 1 to quantify PS in a given frontoparietal or the additional WM circuit (C), for a given adolescent's data. Consistent with Equation 1, the average Euclidean distance between encoding- and delay-period functional connections was calculated. However, each functional connection in a given circuit was made linearly independent from its functional connectivity with the reward node (R; i.e., lesioned) in a given WM phase (e or d), via Pearson partial correlations (cf. Lansink et al., 2008). Thus, pattern stability while lesioning reward node functional connections in a circuit with Q number of brain regions is formalized as

$$PS_{C\,|\,R} = atan^{-1}\left(1 - \left(\frac{\sqrt{(e_{1,2\,|\,R} - d_{1,2\,|\,R})^2 + \dots (e_{Q-1,Q\,|\,R} - d_{Q-1,Q\,|\,R})^2}}{Q}\right)\right) \quad (2)$$

For example, Model $PS_{FP|R}$ estimated the average pattern stability in adolescents' frontoparietal circuit, after each functional connection in this circuit was made linearly independent from its functional connectivity with the reward node. If, on average, frontoparietal pattern stability estimated from Model $PS_{FP|R}$ was less than the actual pattern stability (PS_{FP}), this would suggest that functional connectivity with the reward node significantly increased the stability of neural patterns in adolescents' frontoparietal regions. The same formula and interpretation may be applied to modeling lesions to reward-node connections in the additional WM-circuit regions (Model $PS_{Additional|R}$).

Equation 2 was also adapted to create a supplemental model to test whether lesioning functional connections from other WM-sensitive subcortical regions would produce similar or different pattern stability estimates in frontoparietal regions, compared to Model $PS_{FP|R}$. Three other WM-sensitive subcortical regions were part of the additional WM circuit during the WM task (portions of left and right posterior thalamus, and right cerebellar lobule VII; Figures 2-3, Table 4). Model $PS_{FP|SC}$ estimated the influence of the average of these three subcortical functional connections on frontoparietal pattern stability.

RESULTS

WM Performance

The six WM performance measures entered into the PCA and their descriptive statistics, intercorrelations, and correlations with PC1 are reported in Tables 1 and 2. PC1 accounted for 42% of the variance in WM measures. All measures correlated significantly with PC1 factor scores (r_{range} = .51–.72, $ps < .01$; Table 2). Factor scores on PC1 were used in subsequent analyses as a latent measure of WM performance (WM_L). Consistent with other developmental studies of WM, adolescents' age showed a positive correlation with the WM performance latent variable (WM_L; $p < .05$; Figure 5A); thus, as age increased, WM performance increased as well. Age retained a significant relationship with WM performance latent variable when controlling for sex ($r_{XY|Z}$ = .492, $p = .005$).

IPT and WM Task Activations

Significant IPT (reward > loss) and WM task (WM > rest) activations may be found in Figure 2. Most spatial overlap (81%) between these two tasks occurred within two ventral BG clusters including nucleus accumbens, ventral caudate, and ventromedial putamen (Figures 2-3, Table 3). Coordinates and anatomical labels of functional ROIs from Figure 3 may be found in Tables 3 and 4. Reward and frontoparietal nodes, which were used for our primary hypothesis tests, showed a high degree of spatial overlap with extant functional imaging studies of reward and WM activation, offering confidence in the reproducibility of these nodes in subsequent work (see Supplemental Figures 1-3[1]).

Empirical Analyses: Reward-Frontoparietal Pattern Stability, Age, and WM Performance

We sought to test whether the stability of functional connectivity patterns between reward and frontoparietal WM connections ($PS_{Reward-FP}$) was related to adolescent development by examining its correlation with age. Age was positively associated with pattern stability between reward and frontoparietal WM connections ($PS_{Reward-FP}$; $p < .05$; Figure 5B); thus, as age increased, the stability of functional connectivity patterns between the reward node and frontoparietal regions also increased. We also tested whether pattern stability between reward and frontoparietal WM connections was related to adolescents' WM ability by examining its correlation with our WM performance latent variable (WM_L). The WM performance latent variable was positively associated with adolescents' stability of functional connectivity patterns between reward and frontal parietal regions ($p < .05$; Figure 5C); thus, as adolescents' WM ability increased, the stability of functional connectivity patterns between the reward node and frontoparietal regions also increased.

Relationships between age and the stability of functional connectivity patterns between reward and frontoparietal WM connections ($PS_{Reward-FP}$) retained statistical significance despite controlling for (1) individual differences in the four measures of participant motion, (2) sex, or (3) the use of psychostimulant medication (ps .05; see Supplemental Table 1). Similarly, relationships between the WM performance latent variable (WM_L) and the stability of functional connectivity patterns between reward and frontoparietal

---

[1] All supplemental materials can be retrieved from: https://psychology.unl.edu/nct-lab/resources.

WM connections ($PS_{\text{Reward-FP}}$) retained statistical significance despite controlling for (1) individual differences in the four measures of participant motion, (2) sex, or (3) the use of psychostimulant medication (ps .05; see Supplemental Table 1).

Given the importance of frontoparietal regions for WM, it is possible that examining pattern stability between reward-sensitive BG and these regions might not yield further understanding to WM development, when considering pattern stability in frontoparietal regions more generally. We tested whether the relationship between the stability of functional connectivity patterns between reward and frontoparietal WM connections ($PS_{\text{Reward-FP}}$) and age remained significant after removing the variance accounted for by pattern stability within frontoparietal regions more generally (PS_{FP}). We additionally tested whether the relationship between the stability of functional connectivity patterns between reward and frontoparietal WM connections ($PS_{\text{Reward-FP}}$) and the WM performance variable (WM_{L}) remained significant after removing the variance accounted for by PS_{FP}. Both correlations were attenuated when controlling for the general stability of frontoparietal connectivity patterns (PS_{FP}). However, the stability of functional connectivity patterns between the reward node and frontoparietal regions ($PS_{\text{Reward-FP}}$) still retained a significant relationship with age ($r_{\text{XY|Z}} = .368$, $p = .035$) and WM_{L} ($r_{\text{XY|Z}} = .418$, $p = .019$), despite controlling for PS_{FP}.

We also tested the alternative hypothesis that pattern stability between the reward node and other WM-sensitive regions (i.e., $PS_{\text{Reward-Additional}}$) could be related to adolescent age or WM ability. We failed to find significant relationships between age and pattern stability between the reward node and other WM-sensitive regions ($PS_{\text{Reward-Additional}}$; $r = .084$, $p = .636$). Similarly, we failed to find significant relationships between the WM latent variable (WM_{L}) and pattern stability between the reward node and other WM-sensitive regions ($PS_{\text{Reward-Additional}}$; $r = .293$, $p = .103$). These findings suggesting the stability of goal-relevant patterns between reward-sensitive BG and WM-sensitive frontoparietal regions may be uniquely related to adolescents' age and WM ability.

Computational Analyses: Lesion Models

We hypothesized that, if adolescents' communication between reward-sensitive BG and WM-sensitive frontoparietal regions increased the stability of goal-relevant neural patterns in these frontoparietal regions, then computationally lesioning functional connections with reward-sensitive BG would significantly decrease pattern stability in frontoparietal regions. This hypothesis was supported. Lesioning reward-node functional connections to WM-sensitive frontoparietal regions (Model $PS_{\text{FP|R}}$) significantly decreased pattern stability in frontoparietal regions, compared to no lesioning ($p < .001$; Figure 6A). This result retained significance despite removing variance accounted for by (1) individual differences in the four measures of participant motion, (2) sex, or (3) the use of psychostimulant medication ($ps < .05$; see Supplemental Table 2).

The effects of lesioning reward-node functional connections on frontoparietal pattern stability were dissociated from the general effects of lesioning functional connections from WM-sensitive subcortical regions. Here, we tested whether pattern stability estimates in frontoparietal regions when lesioning the reward node connections (Model $PS_{\text{FP|R}}$) were

significantly less than pattern stability estimates in frontoparietal regions when lesioning connections from other active, subcortical structures (Model $PS_{FP|SC}$). This dissociation was supported (Model $PS_{FP|R}$ < Model $PS_{FP|SC}$, p < .001; Figure 6B); thus, lesioning the reward node connections resulted in significantly less pattern stability in frontoparietal regions relative to lesioning connections from other active subcortical structures. This result retained significance despite removing variance accounted for by (1) individual differences in the four measures of participant motion, (2) sex, or (3) the use of psychostimulant medication (ps < .05; Supplemental Table 3).

The effect of lesioning reward-node connections on pattern stability in WM-sensitive frontoparietal regions was also dissociated from a reward-node lesion model to additional WM-circuit regions. Here, we tested the hypothesis that lesioning reward-node connections would produce significant decreases in frontoparietal pattern stability relative to the effect of lesioning reward-node connections on the pattern stability between the additional WM-circuit regions. This dissociation was supported (p < .001; Figure 6C). Specifically, a repeated-measures ANOVA demonstrated a significant Lesion × Circuit interaction effect on pattern stability; thus, frontoparietal regions showed greater decreases in pattern stability given lesioned reward-node connections, relative to the additional WM-circuit regions given lesions to these same reward-node connections. The Lesion × Circuit interaction retained its significance despite removing variance accounted for by (1) individual differences in the four measures of participant motion, (2) sex, or (3) the use of psychostimulant medication (ps < .05; Supplemental Table 4). The repeated-measures ANOVA also found a main effect of Lesion (partial eta-squared [η_p^2] = .461, p < .001), with reward lesion models showing an overall decrease in pattern stability, compared to pattern stability in these circuits without computational lesioning. There was also a main effect of Circuit (η_p^2 = .355, p = .001), with WM-sensitive frontoparietal regions showing elevated pattern stability relative to the additional WM-circuit regions, which was expected given the proposed role of neural pattern stability in these regions during WM (Frank & Badre, 2011; O'Reilly et al., 2010; Reynolds & O'Reilly, 2009; Gruber et al., 2006; O'Reilly & Frank, 2006).

DISCUSSION

This study sought evidence for reward-driven pattern stability as one possible mechanism explaining the combined significance of BG and frontoparietal regions in adolescent WM development. Empirical analyses revealed that the stability of goal-relevant functional connectivity patterns between reward-sensitive BG and WM-sensitive frontoparietal regions was positively associated with adolescent age and WM ability. These relationships remained significant despite covarying for pattern stability within WM-sensitive frontoparietal regions alone. Relationships failed to reach significance between reward-sensitive BG and the additional WM-circuit regions. Together, empirical results suggest that the extent to which goal-relevant communication patterns within reward-frontoparietal circuitry are maintained (i.e., stability) uniquely increases with adolescent development and WM ability.

Computational lesion modeling revealed that reward-sensitive BG connections increased the stability of goal-relevant connectivity patterns in frontoparietal regions. Two

dissociations were also demonstrated wherein (1) lesions to other active subcortical regions' connections demonstrated significantly less influence on WM-sensitive frontoparietal goal-relevant pattern stability than reward-sensitive BG lesions and (2) reward-sensitive BG lesions showed significantly less influence on goal-relevant pattern stability in active, nonfrontoparietal regions than these lesions did on frontoparietal regions. These analyses cannot inform us in the same manner as actual lesion studies can on the potential causal influence that reward-sensitive BG has on adolescent WM performance. However, consistent with adult models of WM, our computational lesion findings suggest that communication between reward-sensitive BG and frontoparietal regions uniquely increases the stability of goal-relevant neural patterns maintained in adolescents' WM.

The stability of neural patterns across delay periods or task epochs is associated with greater memory performance in adults (Ezzyat & Davachi, 2014; Tambini & Davachi, 2013; see also Sprague, Ester, & Serences, 2016; Stokes, 2016). For instance, in one adult study, the persistence of functional connectivity patterns in hippocampal voxels across encoding and postencoding rest periods (i.e., pattern stability) significantly predicted later memory performance for encoded memoranda (Tambini & Davachi, 2013). In adult neurobiological models of WM, reward-prediction-error signals to and from reward-sensitive BG enhance the stability of encoded neural patterns maintained in WM. However, reward-prediction-error signals must travel throughout a rich circuitry of connections between and within BG as well as prefrontal and parietal cortices. Continued development of these and other circuits until young adulthood (Heller et al., 2016; Simmonds et al., 2014; Lebel & Beaulieu, 2011) and development of this circuit's individual nodes (Davidow et al., 2019; Schrueuders et al., 2018; Wierenga et al., 2018; Satterthwaite et al., 2012, 2013; Somerville et al., 2011) suggest that this circuitry may not be fully capable of stabilizing encoded representations during WM development. Lesser ability to stabilize representations in WM may limit this circuitry's ability to enhance WM performance during development. In support of this hypothesis, our results demonstrated that, as adolescent age increased, encoded neural patterns within reward-frontoparietal circuitry also became more stable. Additionally, by demonstrating a positive relationship with WM performance, our findings suggest that stability within this circuitry may act as one neural mechanism to enhance WM ability during adolescence.

Despite continuing development of cortico-BG circuitry, lesion analyses demonstrated that adolescents' communication signals from reward-sensitive BG are, on average, able to influence the stability of goal-relevant neural patterns in frontoparietal regions. In adult models of WM, reward-prediction-error signals are (directly or indirectly) communicated from reward-sensitive BG to pFC, signaling thalamocortical circuits to "lock the gate" on encoding new information and maintain encoded goal-relevant neural patterns (Frank & Badre, 2011; Gruber et al., 2006; O'Reilly & Frank, 2006). These signals increase the stability of goal-relevant neural patterns within frontoparietal regions, wherein high-level representations of this information are presumed to be maintained (Christophel et al., 2017; D'Esposito & Postle, 2015). Our lesion analyses suggested that communication between reward-sensitive BG and frontoparietal regions plays a similar role in the maintenance of goal-relevant neural patterns in adolescents. However, because the beneficial effects of reward signaling on cognition are not fully realized until young adulthood (Dumotheil et

al., 2011; see also Davidow et al., 2018; Larsen & Luna, 2018), it may be that the extent to which this signaling can be used to stabilize goal-relevant information in frontoparietal regions parallels broader trends in WM and continues development into one's early 20s (e.g., Brockmole & Logie, 2013).

Considerations

Several caveats should be considered in the context of the present work. First, our interpretations and hypotheses are based on neurobiological models of WM, which emphasize the role of BG in reward-prediction-error signaling. More general reward-related processing occurs in many brain regions (e.g., OFC), and future work examining these regions may provide further understanding of reward-related processing in the development of WM (see Davidow et al., 2018; Kahnt, 2017). In addition, the broader function of frontoparietal regions in goal-directed behaviors (Cole, Bassett, Power, Braver, & Petersen, 2014; Miller & Buschman, 2013; Cole & Schneider, 2007; Miller & Cohen, 2001) alludes to the notion that interactions between frontoparietal and reward-related circuitries may play a more expansive role in the development of cognitive domains beyond WM (Davidow et al., 2018; Larsen & Luna, 2018; Luna et al., 2015).

Second, our findings do not supplant the importance of other BG regions' contributions to WM or WM development (e.g., Nemmi et al., 2018; McNab & Klingberg, 2008). In neurobiological models of WM, dorsal and ventral BG have different but complementary functions in enhancing WM maintenance (Frank & Badre, 2011; O'Reilly et al., 2010; Gruber et al., 2006; O'Reilly & Frank, 2006). Although their primary functions are different, communication between these regions is thought to be essential for stabilizing the maintenance of goal-relevant representations in WM (O'Reilly, 2006; O'Reilly & Frank, 2006). For instance, in these models, ventral BG learn which information is goal relevant through interactions with pFC (e.g., error monitoring; Petersen & Dubis, 2012) and other dopaminergic hubs (O'Reilly, 2006; O'Reilly & Frank, 2006). After this learning, reward-prediction-error signals are communicated from ventral BG to dorsal BG, which cue frontoparietal regions to maintain goal-relevant neural patterns. Thus, reward signals from ventral BG are thought to be necessary, but not sufficient, for enhancing the stability of goal-relevant information in WM.

The present results may also be considered in the context of individual variation in development. WM and its neural substrate are sensitive to physiological and social factors during development (e.g., Schulte et al., 2019; Farooqi et al., 2018; Finn et al., 2016; see Larsen & Luna, 2018). This study assessed a young adolescent sample (12.16–14.72 years old) and found that nearly one quarter of the variance in these adolescents' WM abilities could be accounted for by age. Although we present a relatively narrow age range compared to other studies, the observed large-effect-size relationship between age and WM implies a high degree of heterogeneity in WM-related developmental processes in this age group. During adolescence, there are considerable individual differences in WM developmental trajectories (Nemmi et al., 2018; Ullman et al., 2014). There is also evidence for a relatively rapid growth of performance on various measures of WM during early to mid-adolescence, around ages 11–15 years (Montez et al., 2017; Ullman et al., 2014; Brockmole & Logie,

2013; Gathercole et al., 2004; Luciana, Conklin, Hooper, & Yarger, 2005, 2005). Future research should seek to isolate the roles of diverse developmental factors in influencing relationships between age and WM ability, as well as WM ability and goal-relevant pattern stability, during these early adolescent years. For instance, social factors, such as socioeconomic status, have been demonstrated in early adolescence (i.e., middle school students) to have significant relationships with WM performance and frontoparietal brain activations during WM (Finn et al., 2016). Physiological developmental schedules and pubertal onset also vary widely (~2 + years; Patten & Viner, 2007), making an early adolescent age range an ideal target for research to explore such factors as mediators in the relationship between WM performance and neural development.

Conclusion

WM is evident during infancy (O'Gilmore & Johnson, 1995). During adolescence, developmental processes shape and refine this critical cognitive ability (Simmonds et al., 2017; Ullman et al., 2014; Brockmole & Logie, 2013; Satterthwaite et al., 2012, 2013; Crone et al., 2006; Cowan et al., 2005; Gathercole et al., 2004; Barrouillet & Camos, 2001; Towse et al., 1998; see also Davidow et al., 2018; Crone & Steinbeis, 2017; Luna et al., 2015). Because of the relevance of adolescent WM to important outcomes such as scholastic achievement (Finn et al., 2016; Cowan et al., 2005; Gathercole et al., 2004; Gathercole & Pickering, 2000), mental illness (Diwadkar et al., 2011; Ross, Wagner, Heinlein, & Zerbe, 2007; Smith et al., 2006; Martinussen, Hayden, Gohh-Johnson, & Tannock, 2005), and more general adaptive behaviors (Walshe et al., 2019), understanding the combined roles of reward and cognitive-control circuitry on WM may prove important for gaining insights into broader typical and atypical neurocognitive development. Future research employing longitudinal designs and contrasting adolescent pattern stability phenomenon with adult samples are needed to understand the exact nature of how this phenomenon might change through development. However, this study provides the first evidence for reward-driven pattern stability as a functional mechanism to explain how communication between BG and frontoparietal regions may influence WM development.

Supplementary Material

Refer to Web version on PubMed Central for supplementary material.

Acknowledgments

REFERENCES

Achard S, Salvador R, Witcher B, Suckling J, & Bullmore E (2006). A resilient, low-frequency, small-world human brain functional network with highly connected association cortical hubs. Journal of Neuroscience, 26, 63–72. [PubMed: 16399673]

Albert R, Jeong H, & Barabási A (2000). Error and attack tolerance of complex networks. Nature, 46, 378–382.

Atallah HE, Lopez-Paniagua D, Rudy JW, & O'Reilly RC (2007). Separate neural substrates for skill learning and performance in the ventral and dorsal striatum. Nature Neuroscience, 10, 126–131. [PubMed: 17187065]

Baddeley A, Logie R, Bressi S, Della Salla S, & Spinnler H (1986). Dementia and working memory. Quarterly Journal of Experimental Psychology, 38, 603–618.

Barch DM, Burgess GC, Harms MP, Petersen SE, Schlaggar BL, Corbetta M, et al. (2013). Function in the human connectome: Task-fMRI and individual differences in behavior. Neuroimage, 80, 169–189. [PubMed: 23684877]

Barrouillet P, & Camos V (2001). Developmental increase in working memory span: Resource sharing or temporal decay? Journal of Memory and Language, 45, 1–20.

Brockmole JR, & Logie RH (2013). Age-related change in visual working memory: A study of 55,753 participants aged 8–75. Frontiers in Psychology, 4, 12. [PubMed: 23372556]

Casey BJ, Cannonier T, Conley MI, Cohen AO, Barch DM, Heitzeg MM, et al. (2018). The adolescent brain cognitive development (ABCD) study: Imaging acquisition across 21 sites. Developmental Cognitive Neuroscience, 32, 43–54. [PubMed: 29567376]

Christophel TB, Klink PC, Spitzer B, Roelfsema PR, & Haynes JD (2017). The distributed nature of working memory. Trends in Cognitive Sciences, 21, 111–124. [PubMed: 28063661]

Church JA, Bunge SA, Petersen SE, & Schlaggar BL (2017). Preparatory engagement of cognitive control networks increases late in childhood. Cerebral Cortex, 27, 2139–2153. [PubMed: 26972753]

Cole MW, Bassett DS, Power JD, Braver TS, & Petersen SE (2014). Intrinsic and task-evoked network architectures of the human brain. Neuron, 83, 238–251. [PubMed: 24991964]

Cole MW, & Schneider W (2007). The cognitive control network: Integrated cortical regions with dissociable functions. Neuroimage, 37, 343–360. [PubMed: 17553704]

Connolly AC, Guntupalli JS, Gors J, Hanke M, Halchenko YO, Wu YC, et al. (2012). The representation of biological classes in the human brain. Journal of Neuroscience, 32, 2608–2618. [PubMed: 22357845]

Cowan N (2001). The magical number 4 in short-term memory: A reconsideration of mental storage capacity. Behavioral and Brain Sciences, 24, 87–185.

Cowan N, Elliott EM, Saults JS, Morey CC, Mattox S, Hismjatullina A, et al. (2005). On the capacity of attention: Its estimation and its role in working memory and cognitive aptitudes. Cognitive Psychology, 51, 42–100. [PubMed: 16039935]

Cox RW (1996). AFNI: Software for analysis and visualization of functional magnetic resonance neuroimages. Computers and Biomedical Research, 29, 162–173. [PubMed: 8812068]

Crone EA, & Steinbeis N (2017). Neural perspectives on cognitive control development during childhood adolescence. Trends in Cognitive Science, 21, 205–215.

Crone EA, Wendelken C, Donohue S, Van Leijenhorst L, & Bunge SA (2006). Neurocognitive development of the ability to manipulate information in working memory. Proceedings of the National Academy of Sciences, U.S.A, 103, 9315–9320.

D'Esposito M, & Postle BR (2015). The cognitive neuroscience of working memory. Annual Review of Psychology, 66, 115–142.

Daniel TA, Katz JS, & Robinson JL (2016). Delayed match-to-sample in working memory: A brainmap meta-analysis. Biological Psychology, 120, 10–20. [PubMed: 27481545]

Darki F, & Klingberg R (2015). The role of fronto-parietal and fronto-striatal networks in the development of working memory: A longitudinal study. Cerebral Cortex, 25, 1587–1595. [PubMed: 24414278]

Davidow JY, Insel C, & Somerville LH (2018). Adolescent development of value-guided goal pursuit. Trends in Cognitive Sciences, 22, 725–736. [PubMed: 29880333]

Davidow JY, Sheridan MA, Van Dijk KRA, Santillana RM, Snyder J, Vidal Bustamante CM, et al. (2019). Development of prefrontal cortical connectivity and the enduring effect of learned value on cognitive control. Journal of Cognitive Neuroscience, 31, 64–77. [PubMed: 30156503]

De Asis-Cruz J, Bouyssi-Kobar M, Evangelou I, Vezina G, & Limperopoulos C (2015). Functional properties of resting state networks in healthy full-term newborns. Scientific Reports, 5, 1–15.

Delgado MR, Nystrom LE, Fissell C, Noll DC, & Fiez JA (2000). Tracking the hemodynamic responses to reward and punishment in the striatum. Journal of Neurophysiology, 84, 3072–3077. [PubMed: 11110834]

Diwadkar VA, Goradia D, Hosanagar A, Mermon D, Montrose DM, Birmaher B, et al. (2011). Working memory and attention deficits in adolescent offspring of schizophrenia or bipolar patients: Comparing vulnerability markers. Progress in Neuro-Psychopharmacology and Biological Psychiatry, 35, 1349–1354. [PubMed: 21549798]

Dukart J, Holiga S, Chatham C, Hawkins P, Forsyth A, McMillan R, et al. (2018). Cerebral blood flow predicts differential neurotransmitter activity. Scientific Reports, 8, 4074. [PubMed: 29511260]

Dumotheil I, Roggerman C, Ziermans T, Peyrard-Janvid M, Matsson H, Jere J, et al. (2011). Influence of the COMT genotype on working memory and brain activity changes during development. Biological Psychiatry, 70, 222–229. [PubMed: 21514925]

Durstewitz D, Seamans JK, & Sejnowski TJ (2000). Dopamine-mediated stabilization of delay-period activity in a network model of prefrontal cortex. Journal of Neurophysiology, 83, 1733–1750. [PubMed: 10712493]

Eickhoff SB, Paus T, Caspers S, Grosbras MH, Evans AC, Zilles K, et al. (2007). Assignment of functional activation to probabilistic cytoarchitectonic areas revisited. Neuroimage, 36, 511–521. [PubMed: 17499520]

Eickhoff SB, Stephan KE, Mohlberg H, Grefkes C, Fink GR, Amunts K, et al. (2004). A new SPM toolbox for combining probabilistic cytoarchitectonic maps and functional imaging data. Neuroimage, 25, 1325–1335.

Esteban O, Markiewicz CJ, Blair RW, Moodie CA, Isik AI, Erramuzpe A, et al. (2019). fMRIPrep: A robust preprocessing pipeline for functional MRI. Nature Methods, 16, 111–116. [PubMed: 30532080]

Ezzyat Y, & Davachi L (2014). Similarity breeds proximity: Pattern similarity within and across contexts is related to later mnemonic judgments of temporal proximity. Neuron, 81, 1179–1189. [PubMed: 24607235]

Fan L, Li H, Zhuo J, Zhang Y, Wang J, Chen L, et al. (2016). The human brainnetome atlas: A new brain atlas based on connectional architecture. Cerebral Cortex, 26, 3508–3526. [PubMed: 27230218]

Farooqi NAI, Scotti M, Lew JM, Botteron KN, Karama S, McCracken JT, et al. (2018). Role of DHEA and cortisol in prefrontal-amygdalar development and working memory. Psychoneuroendocrinology, 98, 86–94. [PubMed: 30121549]

Finn AS, Minas JE, Leonard JA, Mackey AP, Salvatore J, Goetz C, et al. (2016). Functional brain organization of working memory in adolescents varies in relation to family income and academic achievement. Developmental Science, 20, e12450.

Forbes EE, Brown SM, Kimak M, Ferrell RE, Manuck SB, & Hariri AR (2009). Genertic variation in components of dopamine neurotransmission impacts ventral striatal reactivity associated with impulsivity. Molecular Psychiatry, 14, 60–70. [PubMed: 17893706]

Frank MJ, & Badre D (2011). Mechanisms of hierarchical reinforcement learning in corticostriatal circuits 1: Computational analysis. Cerebral Cortex, 22, 509–526. [PubMed: 21693490]

Gathercole SE, & Pickering SJ (2000). Working memory deficits in children with low achievements in the national curriculum at 7 years of age. British Journal of Educational Psychology, 70, 177–194.

Gathercole SE, Pickering SJ, Ambridge B, & Wearing H (2004). The structure of working memory from 4 to 15 years of age. Developmental Psychology, 40, 177–190. [PubMed: 14979759]

Gruber AJ, Dayan P, Gutkin BS, & Solla SA (2006). Dopamine modulation in the basal ganglia locks the gate to working memory. Journal of Computational Neuroscience, 20, 153–166. [PubMed: 16699839]

Hasselmo ME, & Giocomo LM (2006). Cholinergic modulation of cortical function. Journal of Molecular Neuroscience, 30, 133–136. [PubMed: 17192659]

Author Manuscript

Author Manuscript

Author Manuscript

Author Manuscript

Heller AS, Cohen AO, Dreyfuss MF, & Casey BJ (2016). Changes in cortico-subcortical and subcortico-subcortical connectivity impact cognitive control to emotional cues across development. Social Cognitive and Affective Neuroscience, 11, 1910–1918. [PubMed: 27445212]

Hubbard NA, Hutchinson JL, Motes MA, Shokri-Kojori E, Bennett IJ, Brigante RM, et al. (2014). Central executive dysfunction and deferred prefrontal processing in veterans with gulf war illness. Clinical Psychological Science, 2, 319–327. [PubMed: 25767746]

Hubbard NA, Siless V, Frosch IR, Goncalves M, Lo N, Wang J, et al. (2020). Brain function and clinical characterization in the Boston adolescent Neuroimaging of depression and anxiety study. Neuroimage: Clinical, 27, 102240. [PubMed: 32361633]

Insel C, Kastman EK, Glenn CR, & Somerville LH (2017). Development of corticostriatal connectivity constrains goal-directed behavior during adolescence. Nature Communications, 8, 1605.

Kahnt T (2017). A decade of decoding reward-related fMRI signals and where we go from here. Neuroimage, 180, 324–333. [PubMed: 28587898]

Kriegeskorte N, Mur M, & Bandettini P (2008). Representational similarity analysis-connecting the branches of systems neuroscience. Frontiers in Systems Neuroscience, 2, 4. [PubMed: 19104670]

Lansink CS, Goltstein PM, Lankelma JV, Joosten RN, McNaughton BL, & Pennartz CM (2008). Preferential reactivation of motivationally relevant information in the ventral striatum. Journal of Neuroscience, 28, 6372–6382. [PubMed: 18562607]

Larsen B, & Luna B (2018). Adolescence as a neurobiological critical period for the development of higher-order cognition. Neuroscience & Biobehavioral Reviews, 94, 179–195. [PubMed: 30201220]

Lebel C, & Beaulieu C (2011). Longitudinal development of human brian wriring continues from childhood to adulthood. Journal of Neuroscience, 31, 10937–10947. [PubMed: 21795544]

Leonard JA, Mackey AP, Finn AS, & Gabrieli JD (2015). Differential effects of socioeconomic status on working and procedural memory systems. Frontiers in Human Neuroscience, 9, 554. [PubMed: 26500525]

Li SC, Lindenderber U, & Bäckmann L (2010). Dopaminergic modulation of cognition across the life span. Neuroscience & Biobehavioral Reviews, 34, 625–630. [PubMed: 20152855]

Li SC, Lindenberger U, & Sikström S (2001). Aging cognition: from neuromodulation to representation. Trends in Cognitive Science, 5, 479–486.

Luciana M, Conklin HM, Hooper CJ, & Yarger RS (2005). The development of nonverbal working memory and executive control processes in adolescents. Child Development, 76, 697–712. [PubMed: 15892787]

Luna B, Marek S, Larsen B, Tervo-Clemmens B, & Chahal R (2015). An integrative model of the maturation of cognitive control. Annual Review of Neuroscience, 38, 151–170.

Martinussen R, Hayden J, Gohh-Johnson S, & Tannock R (2005). A meta-analysis of working memory impairments in children with attention-deficit/hyperactivity disorder. Journal of the American Academy of Child & Adolescent Psychiatry, 44, 377–384. [PubMed: 15782085]

May JC, Delgado MR, Dahl RE, Stenger VA, Ryan ND, Fiez JA, et al. (2004). Event-related functional magnetic resonance imaging of reward-related brain circuitry in children and adolescents. Biological Psychiatry, 55, 359–366. [PubMed: 14960288]

McNab F, & Klingberg T (2008). Prefrontal cortex and basal ganglia control access to working memory. Nature Neuroscience, 11, 103–107. [PubMed: 18066057]

Miller EK, & Buschman TJ (2013). Cortical circuits for the control of attention. Current Opinion in Neurobiology, 23, 216–222. [PubMed: 23265963]

Miller EK, & Cohen JD (2001). An integrative theory of prefrontal cortex function. Annual Review of Neuroscience, 24, 167–202.

Mongillo G, Barak O, & Tsodyks M (2008). Synaptic theory of working memory. Science, 319, 1543–1546. [PubMed: 18339943]

Montez DF, Calabro FJ, & Luna B (2017). The expression of established cognitive brain states stabilizes with working memory development. eLife, 6, e25606. [PubMed: 28826493]

Mumford JA, Turner BO, Ashby FG, & Poldrack RA (2012). Deconvolving BOLD activation in event-related designs for multivoxel pattern classification analyses. Neuroimage, 59, 2636–2643. [PubMed: 21924359]

Murray JD, Bernacchia A, Roy NA, Constantinidis C, Romo B, & Wang XJ (2017). Stable population coding for working memory coexists with heterogeneous neural dynamics in prefrontal cortex. Proceedings of the National Academy of Sciences, U.S.A, 114, 394–399.

Nemmi F, Nymberg C, Darki F, Banaschewski T, Bokde ALW, Büchel C, et al. (2018). Interaction between striatal volume and DAT1 polymorphism predicts working memory development during adolescence. Developmental Cognitive Neuroscience, 30, 191–199. [PubMed: 29567584]

O'Doherty J, Dayan P, Schultz J, Deichmann R, Friston K, & Dolan RJ (2014). Dissociable roles of ventral and dorsal striatum in instrumental conditioning. Science, 304, 452–454.

O'Gilmore R, & Johnson MH (1995). Working memory in infancy: Six-month-olds' performance on two versions of the oculomotor delayed response task. Journal of Experimental Child Psychology, 59, 397–418. [PubMed: 7622986]

O'Reilly RC (2006). Biologically based computational models of high-level cognition. Science, 314, 91–94. [PubMed: 17023651]

O'Reilly RC, & Frank MJ (2006). Making working memory work: A computational model of learning in the prefrontal cortex and basal ganglia. Neural Computation, 18, 283–328. [PubMed: 16378516]

O'Reilly RC, Herd SA, & Pauli WM (2010). Computational models of cognitive control. Current Opinion in Neurobiology, 20, 257–261. [PubMed: 20185294]

Patten GC, & Viner R (2007). Pubertal transitions in health. Lancet, 369, 1130–1139. [PubMed: 17398312]

Petersen SE, & Dubis JW (2012). The mixed block/event-related design. Neuroimage, 62, 1177–1184. [PubMed: 22008373]

Pierce JW (2007). PsychoPy—Psychophysicas software in python. Journal of Neuroscience Methods, 162, 8–13. [PubMed: 17254636]

Reynolds JR, & O'Reilly RC (2009). Developing PFC representations using reinforcement learning. Cogntition, 113, 281–292.

Rissman J, Gazzaley A, & D'Esposito M (2004). Measuring functional connectivity during distinct stages of a cognitive task. Neuroimage, 23, 752–763. [PubMed: 15488425]

Ross RG, Wagner B, Heinlein S, & Zerbe GO (2007). The stability of inhibitory and working memory deficits in children and adolescent who are children of parents with schizophrenia. Schizophrenia Bulletin, 34, 47–51. [PubMed: 17873150]

Rypma B, & D'Esposito M (1999). The roles of prefrontal brain regions in components of working memory: Effects of memory load and individual differences. Proceedings of the National Academy of Sciences, U.S.A, 96, 6558–6563.

Rypma B, & D'Esposito M (2000). Isolating the neural mechanisms of age-related changes in human working memory. Nature Neuroscience, 3, 509–515. [PubMed: 10769393]

Rypma B, Prabhakaran V, Desmond JE, Glover GH, & Gabrieli JDE (1999). Load-dependent roles of frontal brain regions in the maintenance of working memory. Neuroimage, 9, 216–226. [PubMed: 9927550]

Satterthwaite TD, Ruparel K, Loughead J, Elliott MA, Gerraty RT, Calkins ME, et al. (2012). Being right is its own reward: Load and performance related ventral striatum activation to correct responses during a working memory task in youth. Neuroimage, 61, 723–729. [PubMed: 22484308]

Satterthwaite TD, Wolf DH, Erus G, Ruparel K, Elliott MA, Gennatas ED, et al. (2013). Functional maturation of the executive system during adolescence. Journal of Neuroscience, 33, 16249–16261. [PubMed: 24107956]

Schrueuders E, Braams BR, Blankenstein NE, Peper JS, Güroglu B, & Crone EA (2018). Contributions of reward sensitivity to ventral striatum activity across adolescence and early adulthood. Child Development, 89, 797–810. [PubMed: 29536503]

Schulte T, Hong J, Sullivan EV, Pfefferbaum A, Backer FC, Chu W, et al. (2019). Effects of age, sex, and puberty on neural efficiency of cognitive and motor control in adolescents. Brain Imaging and Behavior. 10.1007/s11682-019-00075-x.

Shah AM, Grotzinger H, Kaczmarzyk JR, Powell LJ, Yücel MA, Gabrieli JDE, et al. (2019). Fixed and flexible: Dynamic prefrontal activations and working memory capacity relationships vary with memory demand. Cognitive Neuroscience. 10.1080/17588928.2019.1694500.

Siegel JS, Power JD, Dubis JW, Vogel AC, Church JA, Schlaggar BL, et al. (2014). Statistical improvements in functional magnetic resonance imaging analyses produced by censoring high-motion data points. Human Brain Mapping, 35, 1981–1996. [PubMed: 23861343]

Simmonds D, Hallquist MN, Asato M, & Luna B (2014). Developmental states and sex differences of white matter and behavioral development through adolescence: A longitudinal diffusion tensor imaging (DTI) study. Neuroimage, 92, 356–368. [PubMed: 24384150]

Simmonds DJ, Hallquist MN, & Luna B (2017). Protracted development of executive and mnemonic brain systems underlying working memory in adolescence: A longitudinal fMRI study. Neuroimage, 157, 695–704. [PubMed: 28456583]

Smith SM, Jenkinson M, Johansen-Berg H, Rueckert D, Nichols TE, Mackay CE, et al. (2006). Tract-based spatial statistics: Voxelwise analysis of multi-subject diffusion data. Neuroimage, 31, 1487–1505. [PubMed: 16624579]

Somerville LH, Hare T, & Casey BJ (2011). Frontostriatal maturation predicts cognitive control failure to appetitive cues in adolescents. Journal of Cognitive Neuroscience, 23, 2123–2134. [PubMed: 20809855]

Speer ME, Bhanji JP, & Delgado MR (2014). Savoring the past: Positive memories evoke value representations in the striatum. Neuron, 84, 847–856. [PubMed: 25451197]

Sprague TC, Ester EF, & Serences JT (2016). Restoring latent visual working memory representations in human cortex. Neuron, 91, 649–707.

Sternberg S (1966). High-speed scanning in human memory. Science, 153, 652–654. [PubMed: 5939936]

Stokes MG (2016). 'Activity-silent' working memory in prefrontal cortex: A dynamic coding framework. Trends in Cognitive Science, 19, 394–405.

Talairach J, & Tournoux P (1988). A co-planar stereotaxic atlas of the human brain: An approach to medical cerebral imaging. New York: Thieme.

Tambini A, & Davachi L (2013). Persistence of hippocampal multivoxel patterns into postencoding rest is related to memory. Proceedings of the National Academy of Sciences, U.S.A, 110, 19591–19596.

Tisdall MD, Hess AT, Reuter M, Meintjes EM, Fischl B, & van der Kouwe AJ (2012). Volumetric navigators (vNavs) for prospective motion correction and selective reacquisition in neuroanatomical MRI. Magnetic Resonance in Medicine, 68, 389–399. [PubMed: 22213578]

Towse JN, Hitch GJ, & Hutton U (1998). A reevaluation of working memory capacity in children. Journal of Memory and Language, 39, 195–217.

Tricomi EM, Delgado MR, & Fiez JA (2004). Modulation of caudate activity by action contingency. Neuron, 41, 281–292. [PubMed: 14741108]

Tversky A, & Kahneman D (1991). Loss aversion in riskless choice: A reference-dependent model. Quarterly Journal of Economics, 106, 1039–1061.

Ullman H, Almeida R, & Klingberg T (2014). Structural maturation and brain activity predict future working memory capacity during childhood development. Journal of Neuroscience, 34, 1592–1598. [PubMed: 24478343]

Van Essen DC, Ugurbil K, Auerbach E, Barch D, Behrens TE, Bucholz R, et al. (2012). The human connectome project: A data acquisition perspective. Neuroimage, 62, 2222–2231. [PubMed: 22366334]

Walshe EA, Winston FK, Betancourt LM, Khurana A, Arena K, & Romer D (2019). Working memory development and motor vehicle crashes in young drivers. JAMA Network Open, 2, e1911421. [PubMed: 31517969]

Wierenga LM, Bos MGN, Schreuders E, Kamp FV, Peper JS, Tamnes CK, et al. (2018). Unraveling age, puberty and testosterone effect on subcortical brain development across adolescence. Psychoneuroendocrinology, 91, 105–114. [PubMed: 29547741]

Xia M, Wang J, & He Y (2013). BrainNet viewer: A network visualization tool for human brain connectomics. PLoS One, 8, e68910. [PubMed: 23861951]

Zarahn E, Aguirre G, & D'Espositio M (1997). A trial-based experimental design for fMRI. Neuroimage, 6, 122–138. [PubMed: 9299386]

Zhou X, Salinas E, Stanford TR, & Constantinidis C (2016). Dynamic interactions in prefrontal functional connectivity during adolescence. In Wang R & Pan X (Eds.), Advances in cognitive neurodynamics (5th ed.). Singapore: Springer.

Zhou X, Zhu D, Qi X-L, Li S, King SG, Salinas E, et al. (2016). Neural correlates of working memory development in adolescent primates. Nature Communications, 7, 13423.
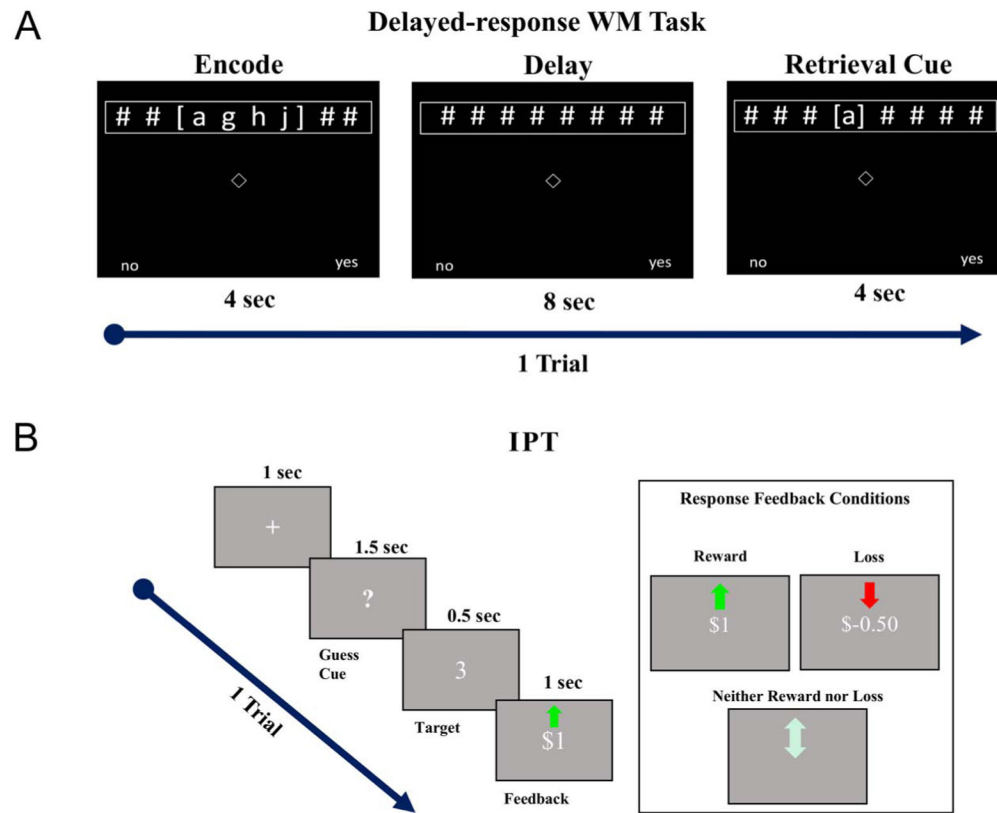
Figure 1.

(A) Example of a single trial of delayed-response WM tasks. Participants were given 4 sec to encode a series of letters (i.e., goal-relevant stimuli). Participants needed to maintain these goal-relevant stimuli over an 8-sec delay period. Participants were then given 4 sec to respond via a dominant-hand, button press (no = index finger, yes = middle finger) whether a retrieval cue-letter matched a letter in the encoded set. Note that perceptual load was balanced across WM task epochs. Participants were instructed only to respond during retrieval cueing. (B) Example of single trial from IPT and different response feedback conditions. Participants were shown a cue and given 1.5 sec to guess whether a forthcoming number (0–9) was greater than or less than 5. Response feedback was experimentally controlled so that task blocks featured either mostly reward or loss feedback.
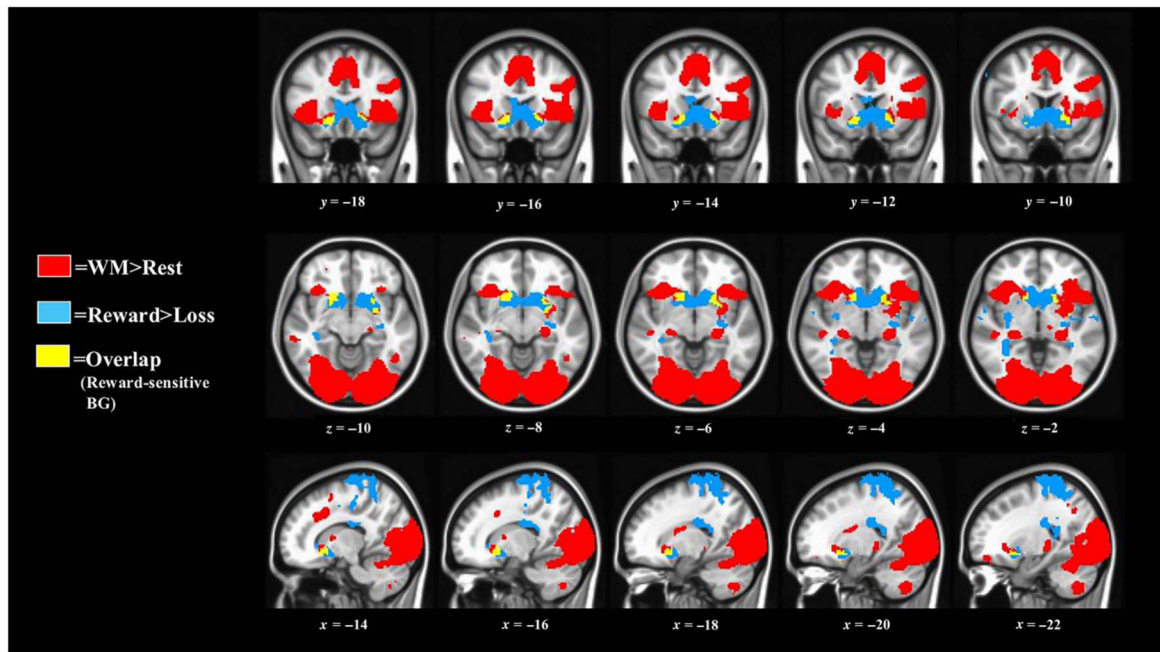
Figure 2.
Significant BOLD activations used to derive the reward node. Reward > loss: $p = .0025$, $k > 99$, FWER < .05. WM > rest: $p = .001$, $k > 70$, FWER < .05. Most (81%) of overlapping voxels were within ventral BG. Three small clusters (5, 12, and 35 voxels; not visible here) also demonstrated overlap between these two tasks.
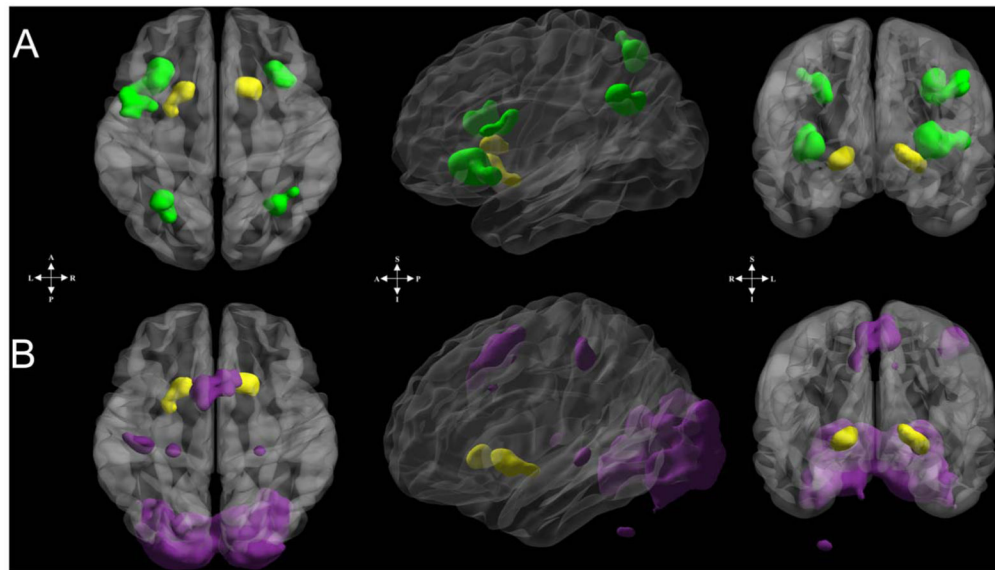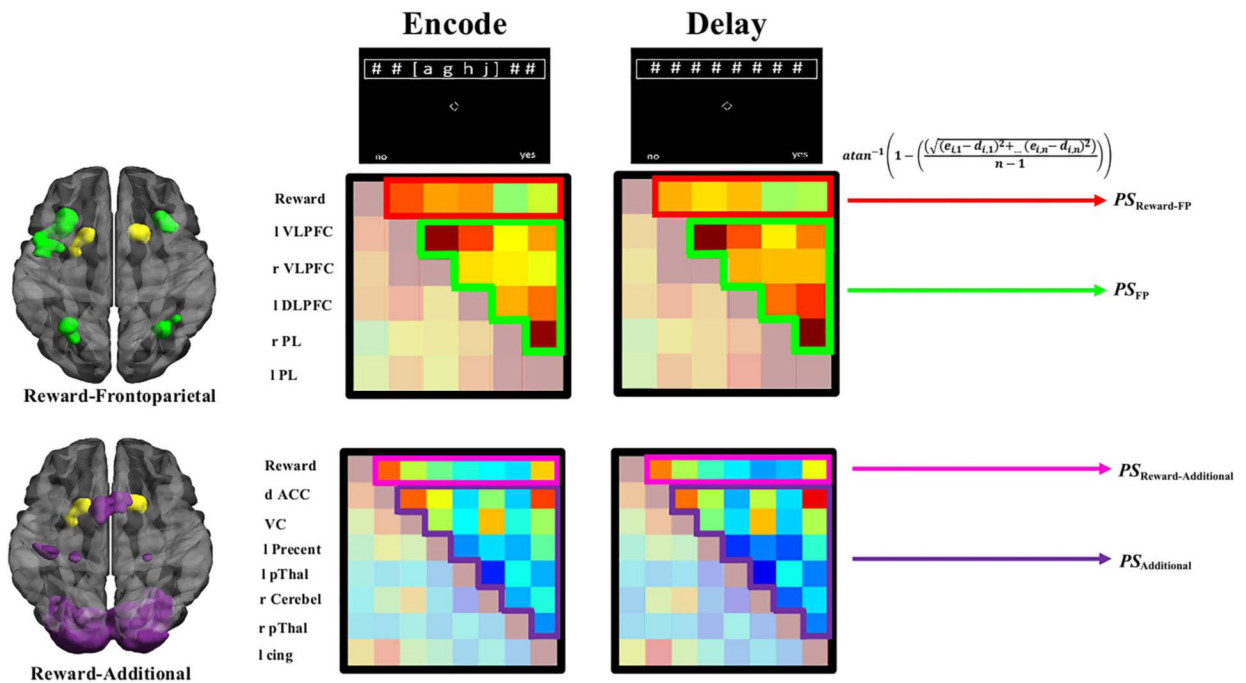
Figure 3.
Reward and WM functional ROIs used in connectivity analyses. (A) Reward node (yellow) and frontoparietal regions (green) comprising the reward-frontoparietal WM circuit. (B) Reward node (yellow) and the additional WM-circuit regions (purple) comprising the reward-additional WM circuit. Nodes in both circuits were derived to ensure no anatomical or functional overlap with the reward node. Regions displayed on surface via box smoothing algorithm employed in BrainNet Viewer (Xia, Wang, & He, 2013). See Tables 3 and 4 for anatomical labels and Montreal Neurological Institute coordinates.

Figure 4.
Conceptual overview of functional connectivity pattern stability estimates by circuit. Reward node (yellow), frontoparietal (FP; green), and additional WM-circuit (purple) nodes comprising different circuits. Example of weighted matrices of correlation patterns by circuit and phase. Emphasized portions of these matrices are input into Equation 1 to derive PS for a given node, for a given participant. Regions (top–bottom): Reward = reward node; l VLPFC = left ventrolateral pFC; r VLPFC = right ventrolateral pFC; l DLPFC = left dorsolateral pFC; r PL = right parietal lobule; l PL = left parietal lobule; d ACC = dorsal ACC; VC = visual cortex; l Precent = left precentral gyrus; l pThal = left posterior thalamaus; r Cerebel = right cerebellar lobule VII; r pThal = right posterior thalamus; l Cingulate = left cingulate. See Tables 3 and 4 for anatomical labels and Montreal Neurological Institute coordinates.
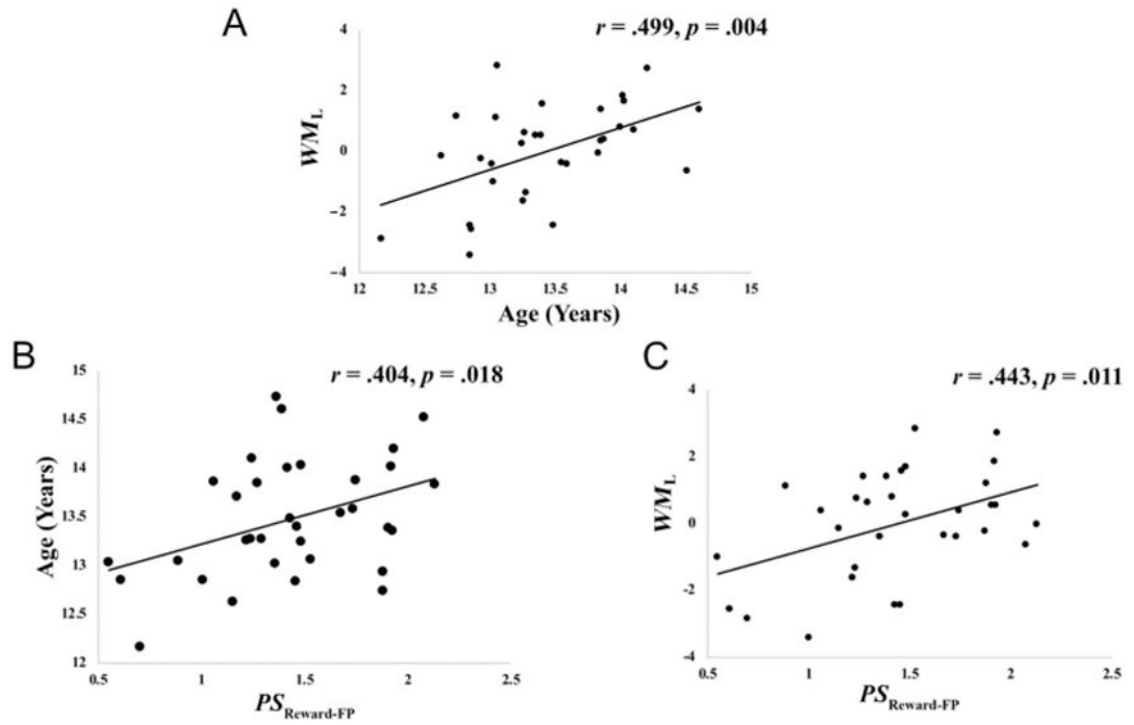
Figure 5.
(A) Association between age (in years) and WM latent factor (WM_L; greater WM_L = greater WM ability). (B) Association between age and functional connectivity pattern stability (greater PS = more stability) in reward-frontoparietal circuit ($PS_{Reward-FP}$). (C) Association between WML and $PS_{Reward-FP}$. These relationships between age and $PS_{Reward-FP}$ (B) and between WM_L and $PS_{Reward-FP}$ (C) retained statistical significance despite controlling for (1) individual differences in the four measures of participant motion, (2) sex, or (3) the use of psychostimulant medication (ps < .05).
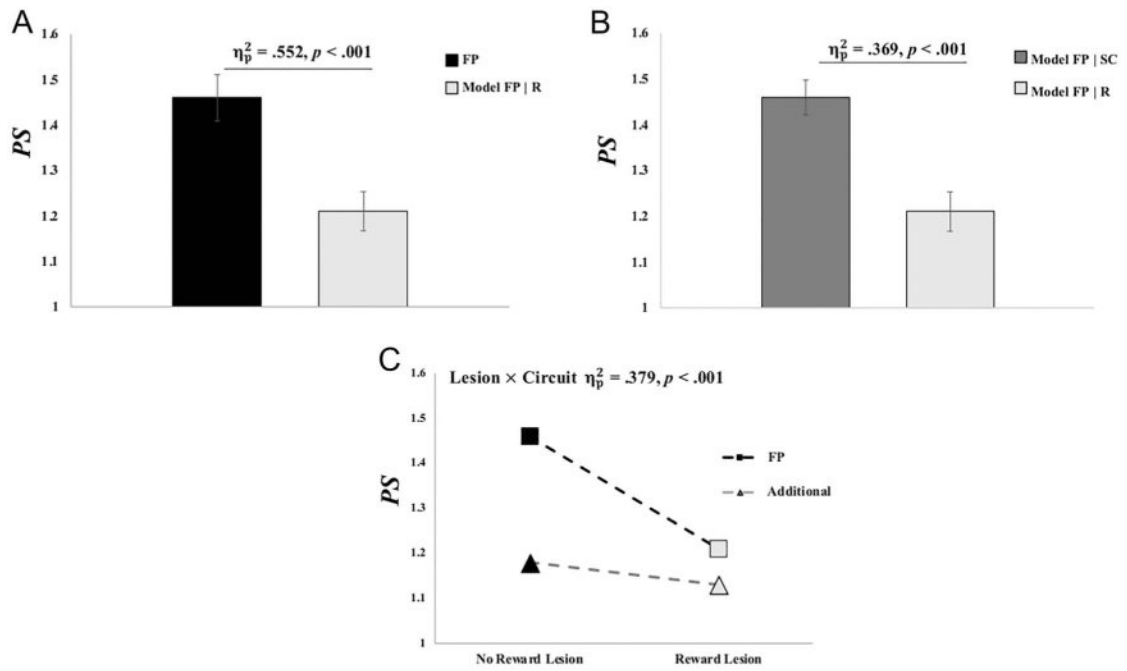
Figure 6.
Lesion model effects on functional connectivity pattern stability (*PS*). (A) Average pattern stability in frontoparietal (FP) regions before (black) and after lesioning connections with the reward node (light gray). (B) Average pattern stability in frontoparietal regions after lesioning connections from the three subcortical WM regions (dark gray) and after lesioning reward node connections (light gray). (C) Effects of lesioning reward node connections on pattern stability in frontoparietal and the additional WM-circuit regions. See main text for other lesion and circuit effects. Error bars reflect 1 *SEM*. η_p^2 = partial eta-squared effect-size estimate from repeated-measures ANOVA. These tests all retained statistical significance despite controlling for (1) individual differences in the four measures of participant motion, (2) sex, or (3) the use of psychostimulant medication (ps < .05).

Table 1.

Descriptive Statistics of Selected WM Performance Measures

Measure	Mean	SEM	Range
Count-span accuracy (%)	59.64	4.19	5.56–94.44
In-scanner WM accuracy (%)	87.66	1.56	68.43–100
In-scanner WM RT (sec)	1.52	0.05	1.11–2.19
n-back accuracy (%)	95.66	0.53	88.88–100
n-back 1-RT (sec)	0.66	0.032	0.33–1.11
Prescan WM capacity (K items)	5.32	1.12	3–7

Six WM measures selected for latent variable (WM_L) analyses and their means, 1 *SEM*, and ranges.

Table 2.

Correlations and Factor Loadings of Selected WM Performance Measures

Measure	1	2	3	4	5	6	PCI
1. Count-span accuracy	–	.13	.30	.43*	.02	.36*	.56***
2. In-scanner WM accuracy	.13	–	.54**	.43*	.36*	.19	.71***
3. In-scanner WM 1-RT	.30	.54**	–	.30	.37*	.38*	.78***
4. *n*-back accuracy	.43*	.43*	.30	–	.29	.29	.72***
5. *n*-back 1-RT	.02	.36*	.37*	.29	–	.02	.51***
6. Prescan WM capacity	.36*	.19	.39*	.29	.02	–	.56***

Six WM measures selected for latent variable (WM_L) analyses and their intercorrelations (see main text for selection details). PC1 = loadings of each measure with Principal Component 1 (i.e., WM_L). RTs were reversed scored for ease of interpretation (1-RT). *p* values, uncorrected.

*
p < .05

**
p < .01

***
p > .001.

Table 3.

Reward-Sensitive BG Clusters, Anatomical Labels, and Coordinates

Cluster	Anatomical Labels	x	y	z	Voxel Count
Right ventral	Nucleus accumbens, ventral caudate	16	17	−06	105
BG	Ventromedial putamen				
Left ventral	Dorsolateral putamen, nucleus accumbens	−22	11	−07	100
BG	Ventral caudate, ventromedial putamen				

Clusters were derived from overlap of significant IPT and WM task activations (see main text). These clusters together comprised the reward node. Coordinates were in Montreal Neurological Institute space (RAI) at the cluster center of mass. All anatomical labels were within 5 mm of the cluster center of mass. Labels were derived from Brainnetome 1.0 Atlas (Fan et al., 2016).

Table 4.

WM Functional ROIs, Anatomical Labels, and Coordinates

Node	Circuit	Anatomical Labels (BAs)	x	y	z	Voxels
VC	Additional	Cuneus, lingual (17, 18)	00	−88	−04	9713
dACC	Additional	Cingulate, medial frontal, superior frontal (6)	00	12	50	728
L VLPFC	Frontoparietal	Inferior frontal, insula (13, 45, 47)	−36	22	03	612
R VLPFC	Frontoparietal	Claustrum, inferior frontal, insula (13, 45, 47)	34	24	00	336
L PL	Frontoparietal	Inferior parietal, precuneus superior parietal (7, 19, 39)	−30	−62	46	282
L Precent	Additional	Postcentral, precentral (2, 3, 4)	−42	−24	54	265
L DLPFC	Frontoparietal	Inferior frontal, middle frontal precentral (6, 9)	−46	04	34	216
R PL	Frontoparietal	Inferior parietal, precuneus superior parietal (7, 40)	34	−60	46	202
L pThal	Additional	Caudal hippocampus, caudal and occipital thalamus, posterior parietal thalamus, rostral temporal thalamus	−24	−28	−04	76
R Cerebel	Additional	Cerebellar Lobule VIIa, VIIb, VIIa crus II	28	−68	−52	54
R pThal	Additional	Caudal hippocampus, lateral prefrontal thalamus, occipital and sensory thalamus, posterior parietal thalamus	24	−28	00	46
L Cingulate	Additional	Anterior cingulate, cingulate gyrus (24, 32)	−12	18	34	27

Nodes were derived from significant clusters of WM activation (see main text). Node abbreviation and circuit designations were listed. Coordinates were in Montreal Neurological Institute space (RAI) at the cluster center of mass. All labels were within 5 mm of the cluster center of mass. Gyrus labels were based on Talairach–Tournoux atlas (Talairach & Tournoux, 1988) with the nearest Brodmann's areas (BAs; within 5 mm) in parentheses. Thalamus labels were derived from Brainnetome 1.0 Atlas (Fan et al., 2016). Cerebellum labels were derived from Eickhoff–Zilles cytoarchitectonic atlas (Eickhoff et al., 2004, 2007).